Static and Dynamic Two-Wave Mixing in GaAs

R. S. Schley, K. L. Telschow and J. Holland

Idaho National Engineering & Environmental Laboratory

Idaho Falls, ID 83415-2209

Abstract

We studied the two-wave mixing anisotropic diffraction process in GaAs for demodulation of static and dynamic phase encoded signals. The static results quantitatively agreed with a previous theoretical model for cubic crystals. This model has been explicitly described for all beam polarizations and crystal rotation angles with respect to the plane of incidence. Dynamic phase modulation, where the signal beam was phase modulated at frequency f_s and the reference beam at $f_r=f_s+\Delta f$, produced a signal at Δf proportional to the difference between the static beam intensities with and without two-wave mixing under all conditions of polarization and crystal orientation studied. A significant dynamic output signal was produced even when only a shift in polarization but no energy transfer occurred as a result of the anisotropic two-wave mixing process. Therefore, not only the two-wave mixing gain is important for using the photorefractive effect for dynamic phase demodulation, but also the polarization shifts occurring from the mixing process.

Key words: Photorefractivity, anisotropic diffraction, two-wave mixing, dynamic phase demodulation, ultrasonic

Introduction

Optical processing of information performed by interfering two waves inside a nonlinear material exhibiting photorefractivity (two-wave mixing) has been extensively studied. Several reviews have been published on the physical effects of two-wave mixing and its many applications[1,2,3,4]. Phase modulation techniques coupled with photorefractivity have produced a large variety of methodologies for modifying and controlling the space charge field and index of refraction grating established in these materials[5,6]. An important application of optical interferometry is the detection of phase modulation impressed on an optical probe beam from scattering off of ultrasonic motion at a surface.[7] Photorefractivity has made an impact on this nondestructive evaluation measurement process through its ability to perform optical phase demodulation through homodyne interferometry from rough and diffusely scattering surfaces.[8,9] The photorefractive process is employed to produce a diffracted reference wavefront with the spatial characteristics of and coaxial with the probe wavefront. Subsequent homodyne interference produces a demodulation of the ultrasonic motion at frequencies greater than the photorefractive cutoff frequency. Another approach is to use the photorefractive process itself to demodulate and image standing waves of a vibrating plate through the two-wave and four-wave mixing processes.[10,11,12,13,14] More, recently, this process has been shown to be able to demodulate and image nonstationary elastic waves in materials.[15]

Most photorefractive materials are crystalline exhibiting anisotropic behavior. Two wave-mixing in these materials is inherently complicated by the tensorial character of the optical properties of these materials. Nevertheless, two-wave mixing can occur in these materials and produce interesting effects, such as cross-polarization coupling, that can be used to

advantage in situations where polarizing components are used to select particular beams from the output.[16] There is a need to quantitatively describe the anisotropic-diffraction process in crystalline photorefractive materials in order to take full advantage of this effect for demodulation of static and dynamic phase information, as suggested above. A nonlinear model of the static photorefractive two-wave mixing in cubic crystals has been developed by Yeh.[17] Gallium Arsenide (GaAs) is a cubic crystal that can be described by this model. Although GaAs has a smaller coupling constant than other photorefractive materials, such as Bismuth Silicon Oxide, its response time is faster making it particularly suitable for ultrasonic measurements. Even though GaAs is optically isotropic, the tensor nature of the electro-optic effect in GaAs crystals allows cross-polarization two-wave coupling. This paper compares the results of two-wave mixing in a GaAs crystal with the predictions of the model developed by Yeh for the static case. In addition to the static case, dynamic modulation at and below a given signal frequency was also investigated. Good agreement was found between the two-wave mixing results and the model for the static case and unusual cross-polarization coupling was observed for the dynamic modulation detection.

Experimental Setup

Two-wave mixing measurements were performed in an undoped GaAs crystal[18] (1 cm x 1 cm x 0.5 cm, absorption coefficient ~ 1.65 cm^{-1}) using a continuous solid state Nd:YAG laser operating at 1064 nm. The experimental configuration and the crystal orientation are shown in figures 1 & 2. The laser beam was split using a polarizing beam splitting cube into signal and reference beams. The signal beam was reflected from a piezoelectrically driven mirror in order to produce a calibrated phase modulation simulating ultrasonic motion. After

exiting the crystal the signal beam passed through a polarization analyzer and filter before entering the photodetector. The reference beam passed through an electro-optic modulator (EOM), and an electronically controlled shutter before mixing with the signal beam in the crystal. The external angle between the beams was 45 degrees resulting in much smaller angle of about 13 degrees within the crystal. Half-wave plates were used to control the polarizations of both beams before entering the GaAs crystal.

The GaAs crystal and the half-wave plates were mounted in manual rotation stages and the polarizer was mounted in a motorized rotational stage. The polarizer was rotated during the experiment to analyze the signal beam after the coupling process occurred. The EOM and vibrating mirror allowed each beam to be phase modulated so that several dynamic signals resulting from the coupling in the crystal could be measured.

Three lock-in amplifiers were used to measure both the static and dynamic aspects of the two-wave mixing process. The output signal from the photodetector was connected to all three lock-in amplifiers. Each lock-in amplifier measured three quantities: the static or dc amplitude and the dynamic signal amplitude and phase. The lock-in measurements corresponded to signals at (1) the signal frequency of the vibrating mirror, 15 kHz, (2) the reference frequency of the EOM, 15.25 kHz, and (3) the difference frequency at 250 Hz.

The crystal orientation and rotation angle, ψ, in the laboratory coordinate system are displayed with respect to the optical beams in figure 2. Definitions of the signal (B_s,B_p) and reference (A_s,A_p) beam polarizations and the crystal coordinates are also shown. A rotation angle of zero degrees for the crystal corresponds to the s-polarization being parallel to the (001) axis of the crystal.

Experimental Procedure:

Prior to starting each experiment the orientation of the crystal and the polarizations of the beams entering the crystal were set. The power of each beam incident on the crystal, the reflections and transmitted power through the crystal were measured and recorded. From this data, the optical absorption coefficient and the reflectivity were measured for each crystal orientation.

Each experiment was performed in three parts. The first part was performed to generate baseline data for the signal beam without beam coupling in the crystal. The driving signal to the vibrating mirror was shut off and the reference beam blocked. The signal beam's transmission through the crystal and polarizer was recorded by the photodetector. During the experiment the polarizer was rotated 360 degrees in 5-degree increments. Since the mirror and the EOM were not modulated, dynamic signals did not exist in this part of the experiment.

The second part of the experiment was performed to determine the static effect of two-wave mixing in the crystal. The reference beam was unblocked allowing beam coupling inside the crystal with the signal beam. The driving signals to the vibrating mirror and the EOM were off, so dynamic signals did not exist.

The third part of the experiment was performed to determine the dynamic effects of two-wave mixing. The reference beam remained unblocked and the driving signals to both the vibrating mirror and EOM were on. With both beams phase modulated, dynamic signals were generated from the beam coupling process.

Typical data from the three parts of one experiment, for a single crystal orientation and set of beam polarizations, are shown in figure 3. Figure 3a shows the static signal beam

intensity without mixing, represented by a solid line, and the static signal beam intensity with two-wave mixing, represented by a dashed line. Figure 3b shows the dynamic signals recorded at the three frequencies: the difference frequency (250 Hz), the signal frequency (15.00 kHz) and the reference frequency (15.25 kHz). The phase was used to determine the sign of the dynamic signal. In the configuration of figure 3, the mixing resulted in energy being transferred from the reference beam to the signal beam. Also, a corresponding large dynamic signal was recorded at the difference frequency. Experiments were conducted for several crystal orientations with various input beam polarizations as depicted in figures 4-7. For the beam polarizations, 0 degrees indicates vertical polarization and positive angles corresponds to clockwise polarization rotation when viewed in the direction of beam propagation (see figure 2). All measurements were taken in the steady state under continuous wave excitation conditions. No fluctuations in the output beam intensities were observed that were beyond those expected from optical phase noise sources present in the laboratory.

Theoretical Static Model:

An anisotropic diffraction model for co-directional two-wave mixing, as developed by Yeh[17], was used to predict the results from the static measurements. This model was extended to account for the two-wave coupling at any crystal orientation angle by considering the geometry and definitions displayed in figure 2. A transformation exists between the two coordinate systems described by

$$\begin{pmatrix} \hat{x} \\ \hat{y} \\ \hat{z} \end{pmatrix} = R(\psi)\begin{pmatrix} \hat{a} \\ \hat{b} \\ \hat{c} \end{pmatrix}, R(\psi) = \frac{1}{\sqrt{2}}\begin{pmatrix} \cos(\psi) & \cos(\psi) & \sqrt{2}\sin(\psi) \\ -\sin(\psi) & -\sin(\psi) & \sqrt{2}\cos(\psi) \\ 1 & -1 & 0 \end{pmatrix}, \quad (1)$$

with $R^{-1}(\psi) = R^T(\psi)$ where R^T is the transpose of the transformation matrix. The optical electric field amplitudes are $\vec{E}_1 = (A_s\hat{s} + A_p\hat{p}_1)\exp(-i(\vec{k}_1 \cdot \vec{r} - 2\pi\nu t))$ and $\vec{E}_2 = (B_s\hat{s} + B_p\hat{p}_2)\exp(-i(\vec{k}_2 \cdot \vec{r} - 2\pi\nu t))$ for the input signal and reference optical beams. The spatial intensity distribution within the crystal is given by the "fringe contrast function" $M(\vec{r}) \equiv \dfrac{\left[\left(A_s^* B_s + A_p^* B_p \cos(2\theta)\right)\exp(-i\vec{K} \cdot \vec{r}) + c.c.\right]}{I_0}$, with $I_0 \equiv A_s^2 + A_p^2 + B_s^2 + B_p^2$, $\vec{K} = \vec{k}_2 - \vec{k}_1 = \left(\dfrac{2\pi}{\lambda}\right)(2\sin(\theta)\hat{x})$, and *c.c.* stands for complex conjugate. The photorefractive process establishes a local electric space charge field $\vec{E}_{sc} = M(\vec{r})\vec{E}_d$, $\vec{E}_d = \left|\vec{E}_d\right|\exp(i\phi)\hat{K}$, $\hat{K} = \dfrac{\vec{K}}{\left|\vec{K}\right|} // \hat{x}$, that is related to the local intensity interference pattern. The local space charge field establishes an optical diffraction grating through the linear electro-optic effect, where ϕ is the phase shift between the intensity interference distribution and the index of refraction grating and E_d is the diffusion field amplitude as described by the band transport model for photorefractivity.[19,20] The external beam angle used resulted in a grating wavelength of about 1.4 μm placing the operation in the diffusive regime. The resulting coupled wave set of equations for all the polarization modes are given as

$$
\begin{aligned}
\frac{d}{dz}A_s &= \frac{i}{2\beta}\exp(i\phi)\left[\Gamma_{ss}\cdot B_s + \Gamma_{sp2}\cdot B_p\right]\cdot M^*(\vec{r})C \\
\frac{d}{dz}B_s &= \frac{i}{2\beta}\exp(-i\phi)\left[\Gamma_{ss}\cdot A_s + \Gamma_{sp1}\cdot A_p\right]\cdot M(\vec{r})C \\
\frac{d}{dz}A_p &= \frac{i}{2\beta}\exp(i\phi)\left[\Gamma_{p1s}\cdot B_s + \Gamma_{p1p2}\cdot B_p\right]\cdot M^*(\vec{r})C \\
\frac{d}{dz}B_p &= \frac{i}{2\beta}\exp(-i\phi)\left[\Gamma_{p2s}\cdot A_s + \Gamma_{p2p1}\cdot A_p\right]\cdot M(\vec{r})C
\end{aligned}
\qquad (2)
$$

where $C = \left(\frac{2\pi}{\lambda}\right)^2 n^4 r_{41} E_q$ and n is the index of refraction, r_{41} is the electro-optic coefficient and ϕ is 90 degrees in the diffusive regime for GaAs.

The electrical permittivity in the presence of a photorefractive grating becomes $\varepsilon = \varepsilon(0) + \Delta\varepsilon(\vec{r})$. For GaAs and other isotropic cubic materials, $\varepsilon_\perp(0) = \varepsilon_{//}(0) = \varepsilon_0 n^2$, $\varepsilon(0) = \varepsilon_0 n^2 \begin{pmatrix} 1 & 0 & 0 \\ 0 & 1 & 0 \\ 0 & 0 & 1 \end{pmatrix}$ and $\Delta\varepsilon(\vec{r}) = -\varepsilon_0^2 n^4 r_{41} \begin{pmatrix} 0 & \vec{E}_{sc}\cdot\hat{c} & \vec{E}_{sc}\cdot\hat{b} \\ \vec{E}_{sc}\cdot\hat{c} & 0 & \vec{E}_{sc}\cdot\hat{a} \\ \vec{E}_{sc}\cdot\hat{b} & \vec{E}_{sc}\cdot\hat{a} & 0 \end{pmatrix}$, in crystal coordinates. In the following, it is assumed that the material can only respond to the space charge field varying slowly in time compared to the optical period and in a direction determined by the Bragg conservation law $\vec{K} = \vec{k}_2 - \vec{k}_1$. From the above, the space charge field can be written for any rotation angle as $\vec{E}_{sc} = \frac{\left|\vec{E}_{sc}\right|}{\sqrt{2}}\left(\cos(\psi)\hat{a} + \cos(\psi)\hat{b} + \sqrt{2}\sin(\psi)\hat{c}\right)$ and the resulting differential permittivity as

$$
\Delta\varepsilon(\hat{r}) = \Delta\varepsilon_m(\hat{r})\frac{1}{\sqrt{2}}\begin{pmatrix} 0 & \sqrt{2}\sin(\psi) & \cos(\psi) \\ \sqrt{2}\sin(\psi) & 0 & \cos(\psi) \\ \cos(\psi) & \cos(\psi) & 0 \end{pmatrix} \qquad (3)
$$

where $\Delta\varepsilon_m(\vec{r}) = -\varepsilon_0 n^4 r_{41} M(\hat{r}) E_q$. The polarization directions $\hat{s}$, $\hat{p}_{1,2}$ can be written in crystal coordinates to produce the following representation for the interaction term coefficients

$$\begin{aligned}
\Gamma_{ss} &= \hat{s}\cdot\Delta\varepsilon(\vec{r})\cdot\hat{s} = \Delta\varepsilon_m(\vec{r})[-\sin(\psi)(3\cos^2(\psi)-1)] \\
\Gamma_{p1p2} &= \Gamma_{p2p1} = \Delta\varepsilon_m(\vec{r})[\sin(\psi)(3\cos^2(\theta)\cos^2(\psi)+\sin^2(\theta)] \\
\Gamma_{sp1} &= \Gamma_{p1s} = \Gamma_{sp2} = \Gamma_{p2s} = \Delta\varepsilon_m(\vec{r})[\cos(\theta)\cos(\psi)(3\cos^2(\psi)-2)]
\end{aligned} \tag{4}$$

where θ is the angle between the beams and the normal to the (-110) face of the crystal as shown in figure 2. With suitable evaluation of the coupling coefficients as a function of the rotated coordinates, the coupled polarization equations (3) were numerically integrated by the Runge-Kutta method to produce the predicted static measurement results[21].

Static results:

Figures 4a-7a show a comparison of the modeling results with the static experimental measurements. A shift in apparent phase on this figure (or equally a shift in polarizer angle) represents a rotation in polarization for that output beam relative to the zero polarization state. In order to compare the predictions of the theory with experiment, the optical absorption coefficient and the two-wave mixing gain coefficient had to be determined. The absorption coefficient was calculated from the measured intensities for each setup. The gain coefficient was determined as that value which produced the best overlap, as judged by eye, of the calculated results with the experimental measurement for the static data of each setup. From these graphs it is seen that the theory (Thy-gain, Thy-nogain) and data (Exp-gain, Exp-nogain) are in good agreement for all the rotation angles of the crystal using the measured values for the attenuation α and the two-wave gain coefficient $\Gamma_B = \dfrac{\pi n^3 r_{41} E_q}{\lambda}$ indicated.

Slight variations of the absorption and gain coefficients were found that are thought to be within experimental error and serve to show a measure of the precision obtained. The theory adequately predicted the polarization shift between the output beam from the mixing and the baseline beam as well as the two-wave gain intensity ratio

$\eta \equiv I_{Bout}(\text{mixing}) \big/ I_{Bout}(\text{no mixing})$. Two-wave mixing theory neglecting anisotropic effects predicts[3]

$$\frac{I_{Bout}(\text{mixing}) - I_{Bout}(\text{no mixing})}{I_{Bout}(\text{no mixing})} = \frac{m(1-\exp(-\Gamma L))}{1+m\exp(-\Gamma L)} \underset{\Gamma L<<1}{\approx} \left(\frac{m}{1+m}\right)\Gamma L, \qquad (5)$$

where $m = \frac{I_{Ain}}{I_{Bin}}$. This result shows that the difference between the static output intensity with and without gain is proportional to the gain coefficient, as can be seen from the data of figures 4a,b.

Dynamic Results:

The dynamic signals at the beam modulation frequencies, result directly from the homodyne interference between those beams and the reference beam produced by the two-wave mixing process. Previous work has described the use of the isotropic two-wave mixing process to produce a coherent reference beam from the signal beam for demodulation of time-varying modulations at frequencies above the crystal response[22]. The subject of this work is the dynamic signal at the difference frequency resulting from the mixing of the signal and reference beams inside the anisotropic GaAs crystal and the subsequent diffraction from the photorefractive grating. The GaAs crystal used had a measured time constant of about 1 ms, corresponding to a cutoff frequency around 1kHz, which was much larger than the 250

Hz difference frequency employed. For the case where no polarization shifts occur (the same as isotropic diffraction) the dynamic wave mixing process can be described by expanding the phase modulated optical electric fields of the interfering beams with a Bessel function series. This produces a static term (proportional to the zero order Bessel function), the first time varying term proportional to the Bessel function of order 1 at the modulation frequency, and higher terms. The first time-varying term in the interference pattern formed from these two beams is proportional to the static term. Therefore, the dynamic differential signal amplitude found from the measurements of figures 4a,b are as expected from a simple extension of the static theory. This was also found in previous work modeling the isotropic dynamic process for detecting traveling ultrasonic waves in materials.[15] The situation is more complicated when anisotropic diffraction occurs, as can be seen from the data of figures 4b-7b which show the difference frequency (250 Hz) signals measured for each configuration. These signals (AC_{exp}) are compared with the difference between the static results with and without two-wave mixing obtained both from the experiment ($Diff_{Exp}$) and from the theoretical modeling ($Diff_{Thy}$). The amplitude of the dynamic signal is dependent on the magnitude of the modulations placed on the signal and reference beams. In order to compare these signals to the static results, the dynamic signals were normalized by the experimental maximum difference between the static intensities with and without two-wave mixing gain. It is interesting to note that the signal at the difference frequency is proportional in amplitude and polarization to the difference between the static signal beam intensity with and without two-wave mixing gain under all conditions tested.

If there is two-wave mixing gain between the static beams with no polarization shift, then a significant dynamic difference frequency signal results as seen in figure 4a,b. In

orientations where there is a polarization shift between the static beams, the dynamic signal goes to zero whenever these signals have the same value. In some cases the maximum amplitude of the static signal with and without gain are the same, indicating no two-wave mixing gain, but a polarization shift is observed. This is the case depicted in figure 5a,b. Here the static beam amplitudes are nearly equal but a polarization shift is present. Figure 6a,b shows that cross polarization conditions exist that exhibit neither energy or polarization transfer, while figure 7a,b shows a condition that includes both. A large difference frequency signal centered around zero voltage offset is recorded showing that anisotropic diffraction can result in a dynamic signal even when the static signals only interact to alter polarizations. This effect of producing a difference frequency signal of significant amplitude when there is little or no exchange of beam energy appears to be a unique consequence of the anisotropic diffraction process. However, the simple application of subtracting the static results with and without two-wave mixing still accurately predicts the dynamic difference frequency signal amplitude and polarization.

The dynamic signals at the vibrating mirror and EOM frequencies shown in figure 3 cannot be predicted from the simple subtraction algorithm that works for the difference frequency signal. The amplitude of the signal at the EOM frequency is not the same as the amplitude at the vibrating mirror frequency. This results from a difference in the modulation depth of the two beams. The phase modulation of the EOM beam was approximately +/- 1 radian. The phase modulation of the signal beam was approximately +/- 0.3 radian. Further analysis of these signals is in progress.

CONCLUSIONS

The anisotropic diffraction process has been studied in detail for the GaAs cubic crystal in both the static and dynamic phase modulation configurations. A detailed theoretical model of the diffraction process has been developed for any crystal orientation from the previously published work of Yeh[17] and compared with experimental measurements for several significant configurations of crystal orientation and input beam polarizations. Excellent agreement between numerical integration of the theoretical model and experimental measurements of the static modulation results were obtained for all the configurations tested. No extension of this model yet exists, to our knowledge, to predict the dynamic modulation results. Experimental measurement of the dynamic modulation diffraction process shows that the diffracted beam at the difference frequency can result with amplitude and polarization determined from the difference between the static beam with and without two-wave mixing. A significant difference frequency signal was recorded for both the case when two-wave mixing gain occurs with resultant energy transfer between the beams and also when only a polarization shift results. The appearance of this latter difference frequency signal due only to the polarization shift is an unanticipated characteristic due to the anisotropic nature of the diffraction process in photorefractive crystals. Future work will extend the numerical modeling to the dynamic modulation measurements.

ACKNOWLEDGMENTS

This work was sponsored by the U.S. Department of Energy, Office of Energy Management under DOE Idaho Operations Office Contract DE-AC07-99ID13727.

FIGURE CAPTIONS

Figure 1. Experimental setup for the anisotropic diffraction two-wave mixing measurements.

Figure 2. Geometrical orientation of the crystal and input optical beams.

Figure 3. Output beam intensities measured as a function of the analyzing polarizer angle for the static (a) and dynamic modulation (b) signals.

Figure 4. Static (a) and dynamic (b) measurement results for the 0° orientation with input signal beam polarization of 45°and reference beam polarization of 45°.

Figure 5. Static (a) and dynamic (b) measurement results for the 0° orientation with input signal beam polarization of 0°and reference beam polarization of 0°.

Figure 6. Static (a) and dynamic (b) measurement results for the 0° orientation with input signal beam polarization of 0°and reference beam polarization of 90°.

Figure 7. Static (a) and dynamic (b) measurement results for the 0° orientation with input signal beam polarization of 45°and reference beam polarization of 0°.

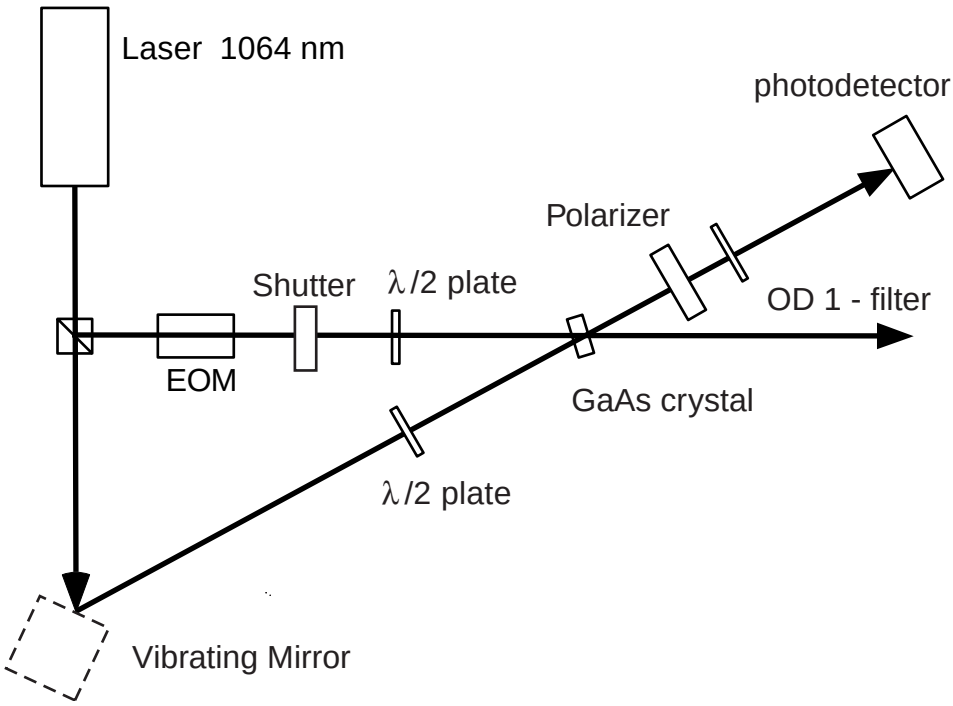

Figure 1. Experimental setup for the anisotropic diffraction two-wave mixing measurements.

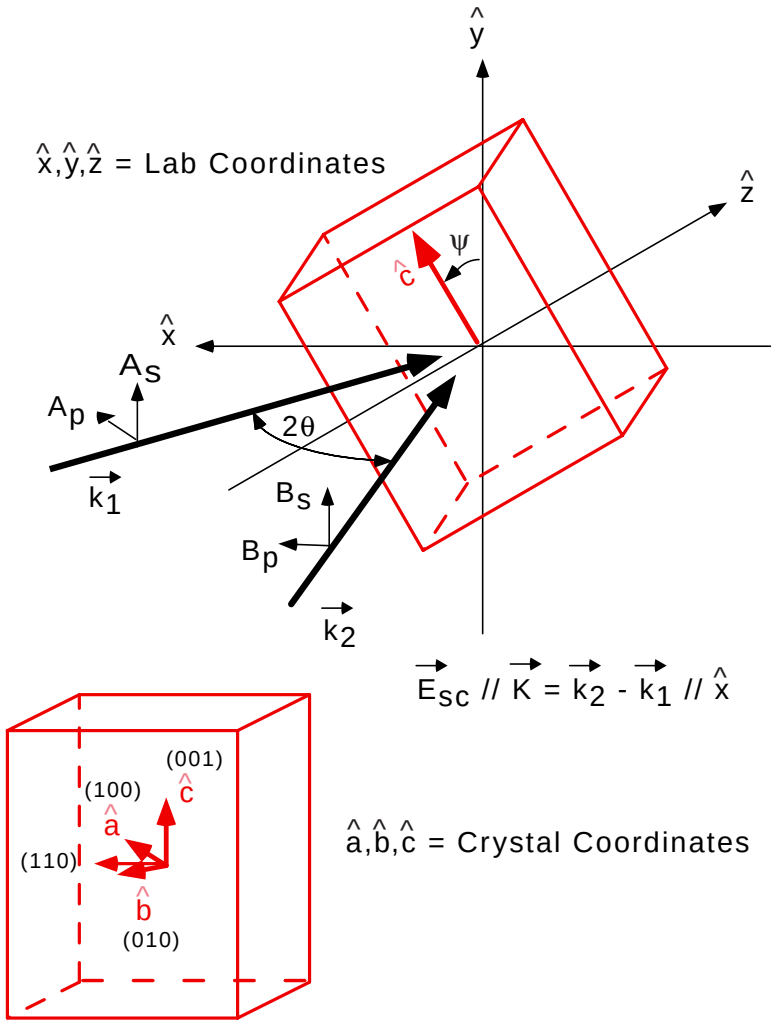

Figure 2. Geometrical orientation of the crystal and input optical beams.

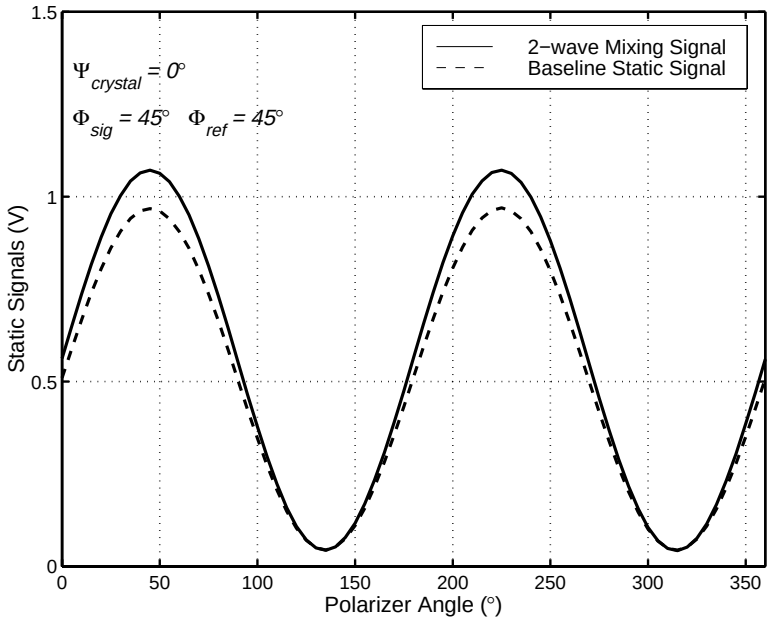

(a)

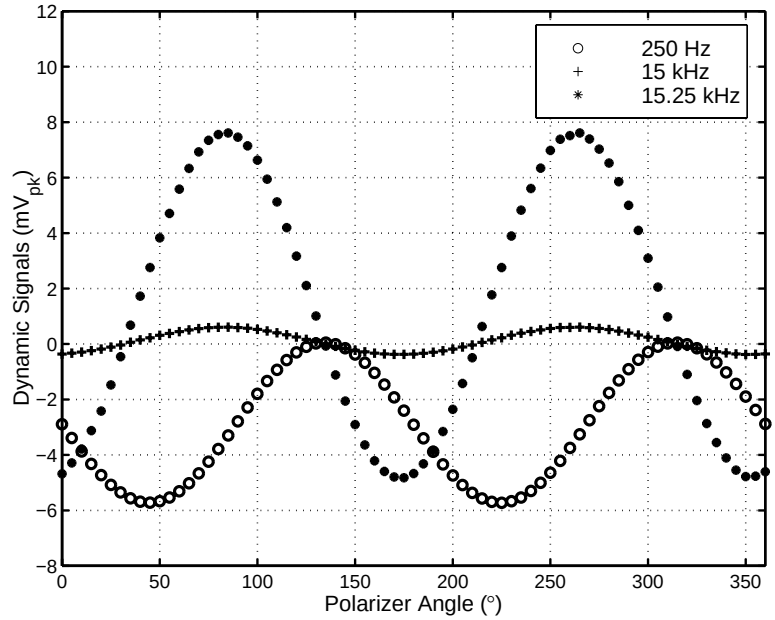

(b)

Figure 3. Output beam intensities measured as a function of the analyzing polarizer angle for the static (a) and dynamic modulation (b) signals.

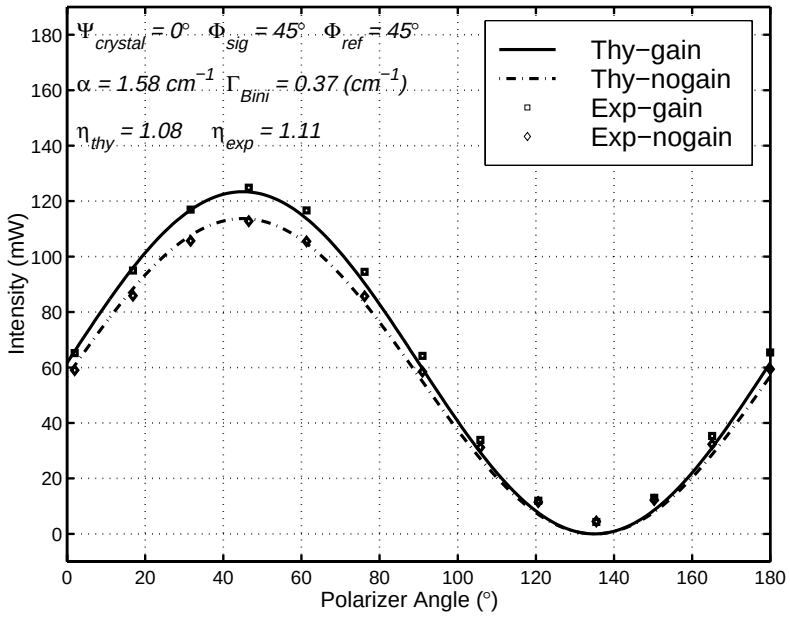

(a)

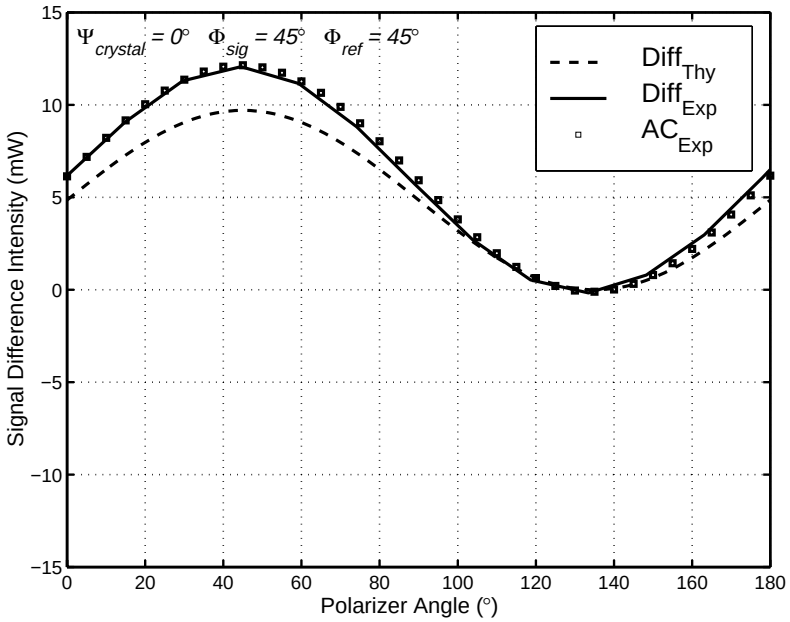

(b)

Figure 4. Static (a) and dynamic (b) measurement results for the 0° orientation with input signal beam polarization of 45°and reference beam polarization of 45°.

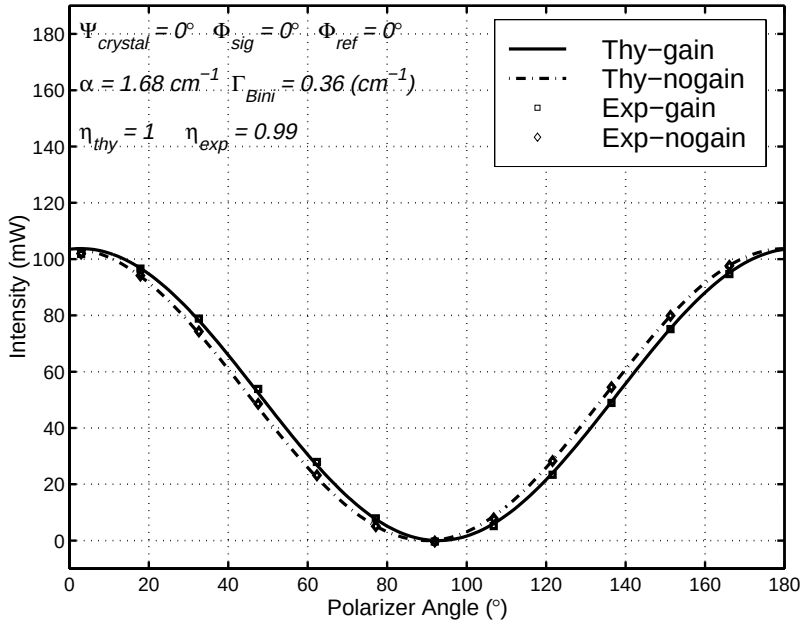

(a)

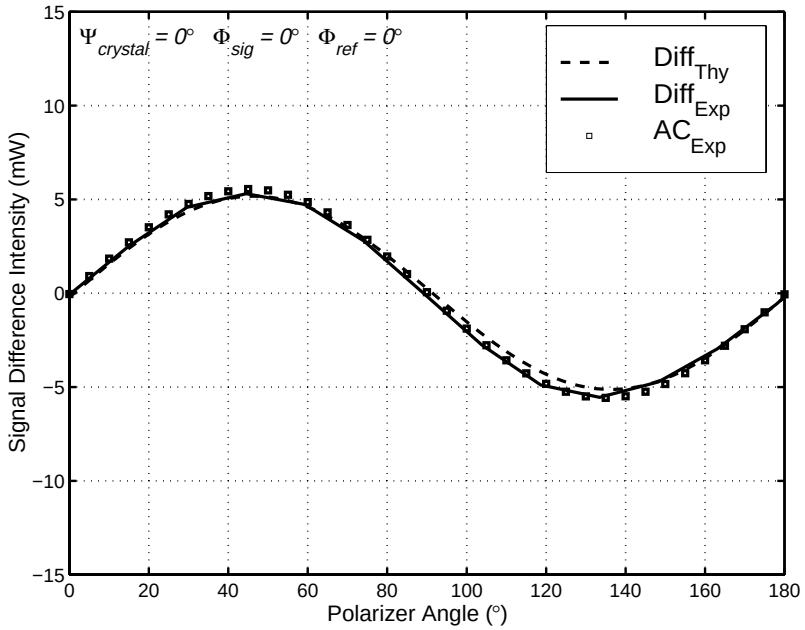

(b)

Figure 5. Static (a) and dynamic (b) measurement results for the 0° orientation with input signal beam polarization of 0°and reference beam polarization of 0°.

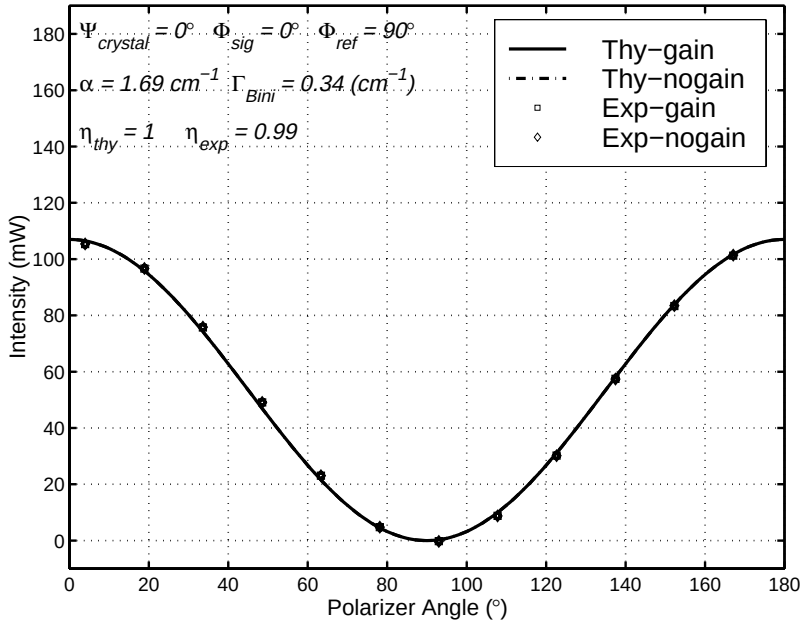

(a)

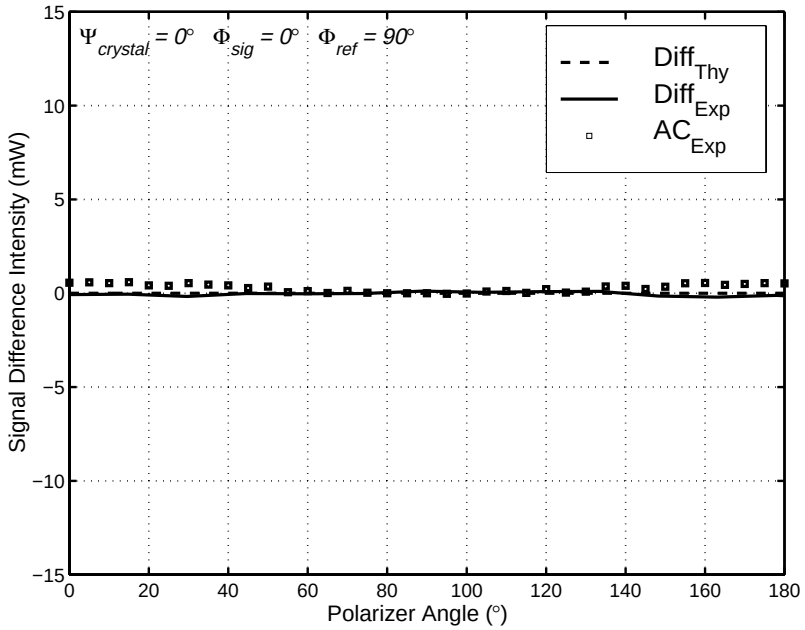

(b)

Figure 6. Static (a) and dynamic (b) measurement results for the 0° orientation with input signal beam polarization of 0°and reference beam polarization of 90°.

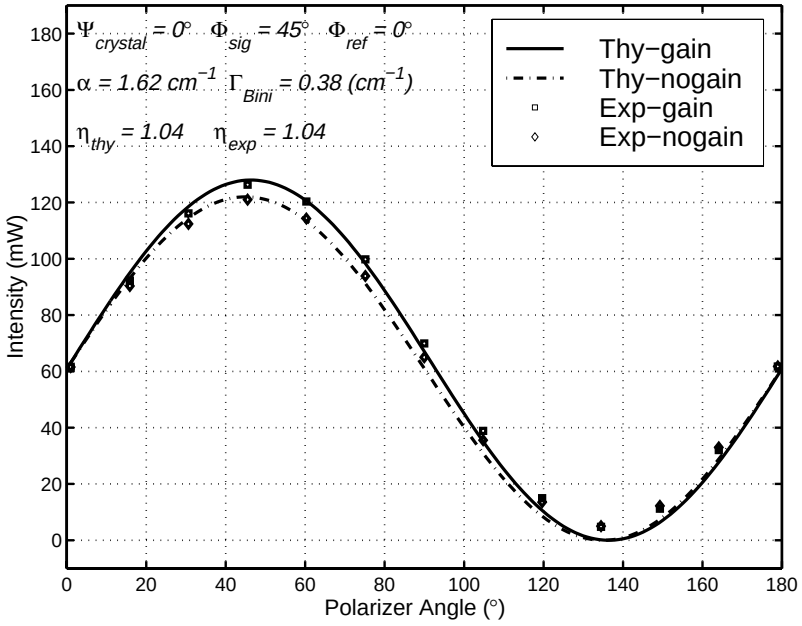

(a)

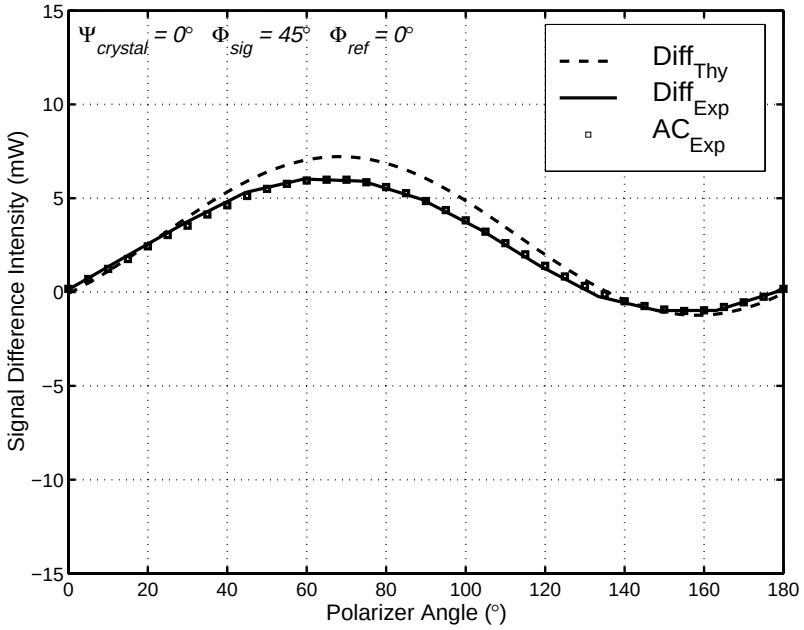

(b)

Figure 7. Static (a) and dynamic (b) measurement results for the 0° orientation with input signal beam polarization of 45°and reference beam polarization of 0°.

REFERENCES

[1] *Electro-optic and Photorefractive Materials*, P. Günter, editor, (Springer-Verlag, New York, 1987)

[2] S. I. Stepanov, *International Trends in Optics*, (Academic Press, New York, 1991) Ch. 9.

[3] P. Yeh, *Introduction to Photorefractive Nonlinear Optics*, (John Wiley, New York, 1993).

[4] *Selected Papers on Photorefractive Materials*, F. M. Davidson, editor, SPIE Milestone Series volume MS 86 (SPIE Bellingham, WA, 1994).

[5] M. Vasnetsov, P. Buchhave, and S. Lyuksyutov, "Phase modulation spectroscopy of space-charge wave resonances in $Bi_{12}SiO_{20}$," Opt. Comm., 137, 181-191 (1997).

[6] J. P. Huignard and A. Marrakchi, "Coherent signal beam amplification in two-wave mixing experiments with photorefractive $Bi_{12}SiO_{20}$ crystals," Opt. Comm. 38, 249-254 (1981).

[7] J. W. Wagner, "Optical Detection of Ultrasound," *Physical Acoustics*, Vol.XIX, Eds. Thurston, R.N., and Pierce, A.D., (Academic Press, New York, 1990) Chp. 5.

[8] G. Hamel de Monchenault and J. P. Huignard, "Two-wave mixing with time-modulated signal in $Bi_{12}SiO_{20}$ theory and application to homodyne wave-front detection," J. Appl. Phys. **63** (3), pp. 624-627 (1988).

[9] R. K. Ing and J.-P. Monchalin, Appl. Phys. Lett. **59**, 3233-3235 (1991).

[10] J. P. Huignard and A. Marrakchi, "Two-wave mixing and energy transfer in $Bi_{12}SiO_{20}$ crystals: application to image amplification and vibration analysis," Opt. Lett., **6**, (12), 622 (1981).

[11] F. Davidson and L. Boutsikaris, “Coherent optical detection through two-wave mixing in photorefractive materials,” Opt. Lett. 13, 506-508 (1988).

[12] H. Rohleder, P. M. Petersen and A. Marrakchi, "Quantitative measurement of the vibrational amplitude and phase in photorefractive time-average interferometry: A comparison with electronic speckle pattern interferometry," J. Appl. Phys., **76** (1), 81-84 (1994).

[13] T.C. Hale and K. Telschow, "Optical lock-in vibration detection using photorefractive frequency domain processing," Appl. Phys. Lett. **69**, 2632-2634 (1996).

[14] T.C. Hale, K.L. Telschow and V. A. Deason, "Photorefractive optical lock-in vibration spectral measurement," Applied Optics, **111**, 8248–8258 (1997).

[15] K.L. Telschow, V. A. Deason, R. S. Schley and S. M. Watson, "Direct Imaging of Lamb Waves in Plates using Photorefractive Dynamic Holography," to be published in the J. Acoust. Soc. Am.

[16] R.C. Troth and J.C. Dainty, "Holographic interferometry using anisotropic self-diffraction in $Bi_{12}SiO_{20}$," Opt. Lett., **16** (1), 53 (1991).

[17] P. Yeh, “Photorefractive two-beam coupling in cubic crystals,” J. Opt. Soc. Am B **4**(9), 1382-1386 (1987).

[18] The GaAs crystal was obtained from Atomergic Chemetals Corporation, 71 Carolyn Boulevard, Farmingdale, New York 11735, Tel: (631) 694-9000, E-mail: info@atomergic.com

[19] N. V. Kukhtarev, V. B. Markov, S. G. Odulov, M. S. Soskin, and V. L. Vinetskii, "Holographic storage in electrooptic crystals. I. steady state," Ferroelectrics **22**, 949-960 (1979).

[20] N. Kukhtarev, P. Buchhave, and S. F. Lyuksyutov, "Optical and electric properties of dynamic holographic gratings with arbitrary contrast," Phys. Rev. A **55**, 3133-3136 (1997).

[21] The Mathworks Inc., Natick, MA 01760-2098, Matlab version 5.2.0

[22] Ph. Delaye, L. A. de Montmorillon, and G. Roosen, "Transmission of time modulated optical signals through an absorbing photorefractive crystal," Opt. Commun. **118**, 154-164 (1995).